Analysis of methods and devices to compress the dynamic range of lidar returns

A.A. Tikhomirov

Institute of Optical Monitoring,
Siberian Branch of the Russian Academy of Sciences, Tomsk

Received December 23, 1999

Classification of methods and devices to compress the dynamic range of lidar returns which includes the regulation elements of optical, photo-electronic, and electronic parts of a lidar receiving system is presented. By the techniques used to regulate the dynamic range the methods are subdivided into the groups that use the logarithmic transformation, compensation for the inverse square-range dependence, and the step-wise change of the gain. A set of criteria to estimate the efficiency of these methods is proposed that includes the compression coefficient, relative increase of sounding distance, conversion accuracy, noise stability, and others. Using these criteria we have carried out comparative analysis of different devices. It is shown that the compression of the dynamic range of return signals in the optical part of the lidar receiving system provides for an increase in the signal-to-noise ratio by several times.

Introduction

The flux of the back-scattered radiation, which is incident on the lidar receiving system, has a wide dynamic range of 6 to 8 orders of magnitude and more. It is the inverse square-range dependence of a return signal and of scattering and absorption of radiation in the atmosphere that cause dynamic range magnitude. When such a signal is recorded losses of useful information occur because there are the lower and upper bounds set of the signal owing to the photons and noise[1] and narrow input dynamic range of a photodetector or a recording device. The input dynamic range $D_{\text{in}}^{\text{ADC}}$ of a modern ADC with the clock frequency 50–100 MHz is no more than 60 dB. The task of optimization is to provide for the best matching of the lidar return power to the magnitude of $D_{\text{in}}^{\text{ADC}}$.

To increase the information content of measurements conducted with systems of laser sounding of the atmosphere, various devices have been developed to compress the dynamic range of lidar return signals $D_{\text{l.s.}}$ at the stage of preliminary signal processing in the receiving system. The review in Ref. 2 presents qualitative analysis of the methods for the $D_{\text{l.s.}}$ compression. Later on, a classification of these methods has been proposed and quantitative criteria for making comparative estimations formulated. Based on them, preliminary analysis of the efficiency of various methods to compress $D_{\text{l.s.}}$ has been performed.

The present paper generalizes the results obtained in this research area for ground-based and airborne lidars.

Dynamic range of lidar returns

In what follows we consider analog mode of lidar return recording. In so doing, let us present its dynamic range by the following expression:

$$D_{\text{l.s.}} = P(z_{\text{i}})/P(z_{\text{f}}) = \frac{z_{\text{f}}^2\, g(z_{\text{i}})\, \beta_\pi(z_{\text{i}})}{z_{\text{i}}^2\, g(z_{\text{f}})\, \beta_\pi(z_{\text{f}})} \times$$

$$\times \exp\left[2 \int_{z_{\text{i}}}^{z_{\text{f}}} \alpha(z)\, \mathrm{d}z\right], \qquad (1)$$

where $P(z_{\text{i}})$ and $P(z_{\text{f}})$ are the maximum and minimum values of the power of scattered radiation flux arriving at the input of the lidar receiving system from the initial z_{i} and final z_{f} distances; $g(z)$ is the value of the geometric factor function which depends on the parameters of a spatial filter[10]; $\beta_\pi(z)$ and $\alpha(z)$ are the coefficients backward and total scattering; $z = ct/2$; c is the speed of light; t is the time from the moment when the sounding pulse has been emitted into the atmosphere.

The values of $D_{\text{l.s.}}$ will be estimated with the allowance for the background noise and the intrinsic noise of a lidar, following Refs. 1 and 11. Let us present the transmission factor of the receiving system (from the input aperture to an ADC) as

$$K_{\text{r.s.}}(t) = g(t)\, K_{\text{t}}\, K_{\text{s}}\, S_{\lambda\text{c}}\, M(t)\, R_{\text{l}}\, K_{\text{a}}(t), \qquad (2)$$

where K_{t} and K_{s} are the transmission of the receiving telescope and spectral filter which are constant in time; $S_{\lambda\text{c}}$ is the spectral response of a PMT's photocathode which is linear relative to the input power over rather a large range of the values $P(z)$[12]; $M(t)$ is the multiplication coefficient of the dynode system; R_{l} is the load resistance of PMT; $K_{\text{a}}(t)$ is the gain of an external amplifier, if any. The coefficients $M(t)$ and $K_{\text{a}}(t)$ can be constant values up to a certain level of the input action or be functions of time which are linear relative to the input signal, if the time-dependent regulation of their values is used, or the functions which are nonlinear relative to the input signal, if the PMT or electronic amplifiers with the logarithmic amplitude characteristics (LAC) are used to compress $D_{\text{l.s.}}$. The coefficient $K_{\text{r.s.}}(t)$ is the multi-parametric value and essentially affects the accuracy of lidar information recording. The dependence $K_{\text{r.s.}}(t)$ on the value of a lidar return and the parameters of receiving system imposes corresponding requirements on the stability and linearity of this coefficient. Below, in considering the devices for compressing $D_{\text{l.s.}}$, by the term "lidar signal" we shall understand either the power of backscattered radiation flux, in the channel from the input aperture of a receiving system to the photocathode of a photodetector, or the electrical signal that is identical to this flux in the channel from the photodetector to the ADC input.

0235-6880/00/02 190-12 $02.00

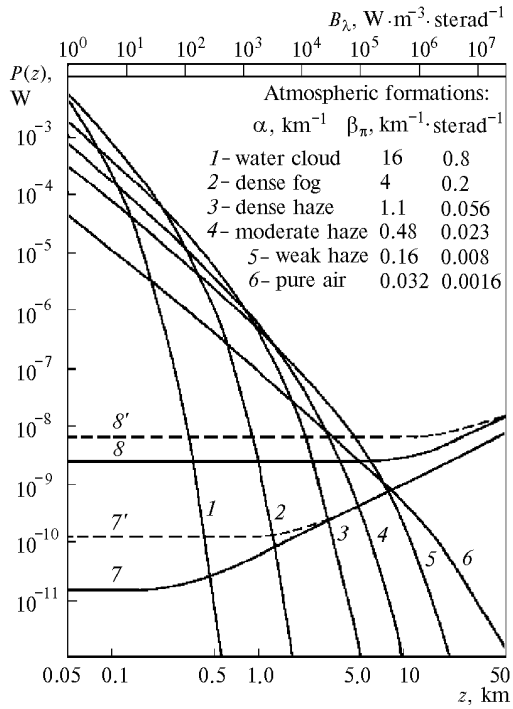

Fig. 1. Possible values of the lidar return signals at the PMT input in sounding homogeneous atmospheric formations.

The curves *1–6* in Fig. 1 show the return power $P(z)$ at the input of a lidar receiving system calculated in a single scattering approximation for different aerosol formations in the atmosphere. The lidar parameters were assumed to be the following: the pulse energy $W_0 = 0.3$ J, pulse duration $\tau_0 = 20$ ns, and the radiation wavelength $\lambda = 694.3$ nm, the area of the receiving telescope $A_t = 0.05$ m^2. If the values of $g(t)$, K_t, and K_s are known the power of the return signal at the photodetector can be determined. The curves *7* and *8* depict the equivalent threshold powers $P_{th.e}$[13] of two specific PMT types (PMT–84 and PMT–83, respectively):

$$P'_{th.e} = P_{th.c} + P_{th.b} = 2eM^2 \Delta f [I_{cc} + S_{\lambda c} N]. \quad (3)$$

Here $P_{th.c}$ and $P_{th.b}$ are the threshold powers determined by the photocathode dark current I_{cc} and external background having the power $N = B_\lambda A_t \Omega_{th} K_t K_c \Delta\lambda$ at the PMT input. B_λ is the spectral brightness of the background, its scale is presented at the top part of the figure; $\Omega_{th} = 4.9 \cdot 10^{-6}$ steradian is the solid angle. $K_t K_s = 0.2$; $\Delta\lambda = 1$ nm is the bandwidth of the spectral filter; the multiplication coefficient M equals to $4 \cdot 10^5$ for PMT–83 and 10^6 for PMT–84. For a more accurate estimation of the equivalent threshold power it is necessary to take into account the contribution of the shot noise of the signal current $I_s = S_{\lambda c} M \Phi(t)$, its root-mean-square component equals to $i_s(t) = M\sqrt{2eS_{\lambda c}\hat{O}(t)\Delta f}$, where $\Phi(t) = g(t)K_t K_s P(t)$, e is the electron charge, Δf is the bandwidth of the electronics channel. Assuming the condition $P_{th.s} = \Phi(z_f)$ to be satisfied at the far end of a sounding path, we find $P_{th.s} = 2e\Delta f / S_{\lambda c}$. The dashed curves *7′* and *8′* in Fig. 1 correspond to the threshold powers $P_{th.e} = P_{th.s} + P_{th.b} + P_{th.c}$ which take into account total noise that sets a lower bound on $D_{l.s}$. Given the value of B_λ one can determine the level of $P_{th.e}$ by relations *7′* and *8′* for a particular PMT, and then using the value $P_{th.e}$ one can find, with the help of curves *1–6* in Fig. 1, the theoretical limit for the maximum achievable sounding distance in the corresponding meteorological formation assuming the signal-to-noise ratio to be unity. By setting the signal-to-noise ratio at the PMT input to be equal to 5–10, one can determine the sounding distance z_f which is potentially achievable and, correspondingly, the limiting value of $D_{l.s.}$.

Classification of the methods

For the design of a lidar system the choice of specific instrumental technique to compress $D_{l.s.}$ requires comparative estimation of their efficiencies according to the quality criteria.[14] Following the classification[3,4] proposed (Table 1), the $D_{l.s.}$ compression methods and instrumentation for their realization are divided into two large classes: active and passive ones. In this case, following Ref. 15, the methods that require an additional power supply to compress $D_{l.s.}$ are related to the first class. Then the methods are subdivided into three sub-classes according to the operation principle used: the optical, photoelectronic, and electronic ones.

Besides, all methods are divided into two groups: single-pulse and multipulse methods. It is characteristic of one group that the $D_{l.s.}$ compression is such that the return signal from the entire sounding path can be recorded from a single sounding pulse. In using the methods from the other group, several sounding pulses are needed for the sounding path to be investigated. From the first pulse the signal is recorded from the near zone of the path, from the second pulse the signal is recorded from the next part and so on.

Table 1. Generalized classification of the methods to compress the lidar return dynamic range

<table>
<tr><td rowspan="2">Methods</td><td rowspan="2">Type of regulation</td><td colspan="3">Passive</td><td colspan="3">Active</td></tr>
<tr><td colspan="3">Optical</td><td colspan="2">Photoelectronic</td><td>Electronic</td></tr>
<tr><td rowspan="4">Single pulse</td><td rowspan="3">Functional linear</td><td rowspan="2">Vignetting diaphragms</td><td>with simple form</td><td rowspan="2">–</td><td rowspan="3">PMT TDA by the t^2 law</td><td>Regulation by the modulator</td><td rowspan="3">Amplifier with t^2 TDA</td></tr>
<tr><td>compensating t^2</td><td>Regulation by the dynodes</td></tr>
<tr><td>Elements compensating t^2</td><td>optical wedges
mirrors</td><td>Electro-optical shutter</td><td>Regulation by supply voltage</td></tr>
<tr><td>Functional nonlinear</td><td colspan="3">–</td><td colspan="2">Logarithmic PMT</td><td>Logarithmic amplifier</td></tr>
<tr><td></td><td colspan="2">Several receiving systems
Several sounding beams</td><td></td><td colspan="2">PMT with a step-wise TDA</td><td>Amplifier with TDA</td></tr>
</table>

Multi-pulse	Step-wise	Receiving system with several photodetectors	–	Reading out signals from load resistors of the dynodes	step-wise regulation of the amplification
		Accessory neutral filters		PMT with switching of the gain	Amplifier with the step-wise switching of the gain
		Accessory field diaphragms			
	Gating	Mechanical shutter	Electro-optical shutter	Gated PMT	Gated amplifier

By the type of the signal regulation used, the following subgroups can be separated out from these methods:

a) the functional continuous control: by multiplying of received signal by the squared range (time) or taking logarithm of the signal;

b) the step-wise control, when the sensitivity of the recording system is kept constant within one part of the sounding path, and then it is increased by a step when a return signal decreases down to some preset value;

c) the gating, when echo-signals are recorded at a constant sensitivity over some range (time) interval.

Although in rigorous mathematical interpretation the methods of both the first and the second sub-groups are functional, below we shall use the term "functional" only in application to the first subgroup. The second subgroup we shall call "step-wise". Let us separate the methods of active linear and nonlinear functional control. In the first case the $D_{\text{l.s}}$ compression is carried out with controlled functional elements when in addition to lidar signal some regulation action is applied to these elements, and these elements remain linear with respect to input signal up to a certain level of the lidar return signal. The PMTs and electronic amplifiers with the time dependent regulation of the amplification (TDA) are to be mentioned among them. In the second case the gain of functional element (the regulation law) depends on the value of lidar return signal affecting it. And at certain levels of the latter a PMT or an amplifier have the logarithmic amplitude characteristic (LAC).

In Table 1 the primary attention is given to the optical and photoelectronic methods as more promising for use in lidar systems. Moreover, a comprehensive description of methods to compress the dynamic range of electrical signals can be found in the Ref. 15. It is obvious that the compression of $D_{\text{l.s.}}$ in the optical or photoelectronic channels is preferable since the signals with lower amplitude will arrive at the next parts of the recording system.

Let us consider some engineering aspects of the $D_{\text{l.s.}}$ compression methods presented briefly in Table 1. The spatial filters (vignetting diaphragms, optical films, wedges, and mirrors) are the passive functional elements and realize the linear attenuation of lidar returns according to some preset law.[9,10] In the blind zone of a lidar, when $g(z) = 0$, no signal from the scattering volume arrives at the photodetector. In the transient zone the vignetting of the backscattered radiation flux by a field-stop diaphragm decreases and the part of light flux that reaches photodetector increases. When $g(z)$ takes the unity value the whole radiation flux which has arrived at the input aperture of the receiving system passes completely through the diaphragm. By varying its sizes and location, one can change the fraction of a lidar return power that reaches the photodetector.[10] It is an essential disadvantage of this approach that information on the nearest layers of the atmosphere is lost, that can affect the accuracy of the obtained results. Certain specific spatial filters compensating for the inverse square-range fall off of a lidar return have been considered in Ref. 10.

The multitelescope receiving system[16] realizes the step-wise regulation in the optical channel of a lidar. Two and more receiving systems of different diameters and field-of-view angles placed at different distances from the transmitter allow the entire $D_{\text{l.s.}}$ range required and the agreement between $D_{\text{l.s}i}$ and $D_{\text{in}i}^{\text{ADC}}$ to be achieved in every receiver in each lidar return. Another realization of the step-wise regulation in the optical channel is to use several sounding beams[17] which cross the optical axis of a receiver at different distances from the lidar.

The use of several photodetectors in receiving system which are switched at different times allows one to realize also the step-wise regulation, although such a method is more close to the gating of the photodetector. The use of several PMTs in one receiving system in combination with the constant optical attenuators that are placed before them is an example of the step-wise regulation of $D_{\text{l.s}}$ also. A set of changeable neutral density filters and field-stop diaphragms, while one PMT, allows one to change step-wise the sensitivity of recording system for different parts of the path and it is used in the multipulse sounding.

The electrooptical switch can realize the controlled attenuation of a signal and its gating depending on the shape of control voltage. Its disadvantage is the small range of the gain regulation ($K_{\max}/K_{\min} < 20$).

The high-speed synchronous mechanical shutter, which is placed before the photodetector cuts signals from the near zone of a sounding path. With the neutral density filters the signals exceeding the maximum permissible level, for a particular photodetector used, are attenuated. By changing the time delay of cut and the filters one can sound by parts the entire path. This method is used in lidars for high-altitude sounding of the atmosphere. It is possible to use, for these purpose, high-speed gated PMTs. However, to study fast atmospheric processes, all these devices can be used for the multipulse sounding only.

To realize the algorithm of processing according to the law $S(z) = p(z)z^2$ (Refs. 18 and 19), the correction of a signal for the inverse squared range (time) in different parts of receiving system is used.[10,16,20] The logarithmic transformation of a signal is realized in the photo-electronic and electronic amplification channels.[15,23] In amplifiers this conversion is frequently carried out jointly with the signal correction by summing with the voltage varying by $2\ln(z)$ law that is equivalent to the algorithm of $\ln[P(z)z^2]$.

Using the step-wise TDA of PMT the multiplication coefficient $M(t)$ for the remote parts of the path increases abruptly in the photoelectronic channel. The recording of signals from the dynode load resistors[24] is used also. In

some lidars the amplifiers with the step-wise switch of the gain have been used.[25]

A set of quality estimation criteria

To compare the different devices intended for compressing $D_{l.s.}$, the following criteria of their efficiency estimation have been proposed[3,5]: the coefficient of the dynamic range compression; the range interval where the compression is being performed; the relative increase in the range of sounding; the error of signal conversion; the noise stability. The following characteristics are referred to as additional ones: the responsiveness and reliability; the design factor, aspect ratio, and costs.

The coefficient of the dynamic range compression. The regulation element of the receiving system, that compresses $D_{l.s.}$, is described by the regulation characteristic[15]

$$V = f(F), \tag{4}$$

where V is the output effect of the input action F. The input action for optical channel is the power $P(t)$, for a photodetector it is $\Phi(t)$, and for an amplifier it is the voltage $U(t)$. For an optical channel the output effect equals to $\Phi(t)$, and for a photodetector and amplifier it equals to the voltage of an electrical signal $U(t)$.

The dynamic range of the regulation element in response to the input action is

$$D_{in} = F(t_i)/F(t_f), \tag{5}$$

where $F(t_i)$ and $F(t_f)$ are the input actions at the time moments t_i and t_f corresponding to the beginning and the end of the signal regulation.

In optical channel the value $F(t_i)$ is determined by the parameters of transmitting-receiving system, and $F(t_f)$ is determined by the transmission gain of spatial filter[9,10] or by the minimal level of the power that is recorded by a photodetector at the noise level (see Fig. 1). For a photodetector the action $F(t_i)$ is determined by the maximum permissible response of the pulse current which is a photodetector specification, and $F(t_f)$ characterizes the minimum value of power at which the regulation amplitude characteristic (LAC in the case of nonlinear photodetector) starts, or the minimum value of power, which allows a signal at the noise level to be recorded (for a linear photodetector), or determines the value of a signal at the time moment t_f corresponding to the TDA termination.[20] For a logarithmic amplifier $F(t_f)$ is determined by the input voltage corresponding to the beginning of LAC, and $F(t_i)$ is determined by the voltage corresponding to its end. For an electronic amplifier with TDA the $F(t_i)$ and $F(t_f)$ are determined in the same way as the TDA of a PMT.

The dynamic range of a signal at the regulation element output is determined as

$$D_{out} = V(t_i)/V(t_f), \tag{6}$$

where the responses $V(t_i)$ and $V(t_f)$ correspond to the input actions $F(t_i)$ and $F(t_f)$ according to (4). The instrumental coefficient of the $D_{l.s.}$ compression equals to

$$G = D_{in}/D_{out}. \tag{7}$$

The larger the achieved value of G, the higher is the efficiency of the method.

The sounding range interval and its relative increase are determined from the condition of optimal matching of the input dynamic range of an ADC D_{in}^{ADC} with the output dynamic range of the recording system $D_{out}^{r.s.}$

$$D_{in}^{ADC} = D_{out}^{r.s.}. \tag{8}$$

Let us introduce the value $\xi = z_f/z_i$ that characterizes the maximum possible interval of the sounding range at $D_{l.s}$ compression. It is a function of the coefficient G and depends on the characteristics of a regulation element. To make a comparison among the compression methods and to compare their efficiency with that of lidar return transfer without any regulation ($G = 1$), it is convenient to use the concept of a relative increase in the sounding range.

$$\delta z = \xi(G)/\xi(1) = z_{fG}/z_{f.l}, \tag{9}$$

where z_{fG} and $z_{f.l}$ are the maximum sounding ranges achievable using the $D_{l.s}$ compression and without it, respectively. The relation (9) determines the maximum possible (theoretical) estimation of the method by the increase in the interval of sounding ranges.

The error of a lidar return conversion by a regulation element is an essential factor in sounding when the quantitative information is determined directly from the signal profile. In such sounding problems as cloud boundary ranging or other sounding problems that use relative amplitude measurements of signals at different wavelengths that passed through the same regulation element requirements to the signal conversion errors are lowered.

This error is determined by the deviation $\Delta V(t)$ of an actual regulation characteristic $f(F)$ from the preset law of a functional transformation $\varphi(F)$:

$$\Delta V(t) = f[F(t)] - \varphi[F(t)], \tag{10}$$

and also by the relative value of this deviation

$$\delta V(t) = \Delta V(t)/\varphi[F(t)]. \tag{11}$$

The values $\Delta V(t)$ and $\delta V(t)$ depend on the signal amplitude, time of the regulation, and other factors depending on the type of regulation element used and its effect on the value of the transmission gain $K_{r.s.}(t)$ determined by the expression (2).

Noise stability. According to this criterion, the effectiveness is determined by an increase in the signal-to-noise ratio and is characterized by the value $[D_{SN}(t)]_G/[D_{SN}(t)]_1$, where $[D_{SN}(t)]_G$ and $[D_{SN}(t)]_1$ are the signal-to-noise ratios in the cases when some method of the dynamic range compression is used and without the use of any. Since the value of a lidar return signal continuously changes with range, the concept of the dynamic signal-to-noise ratio have been introduced[8]:

$$D_{SN}(t) = \frac{\overline{I_s^2(t)}}{\overline{i_n^2(t)}} = \tag{12}$$

$$= \frac{[K_t K_s g(t) S_{\lambda C} A_t W_0 \beta_\pi(t) T^2(t) t^{-2}/c]^2}{2e\Delta f \{K_t K_s S_{\lambda C} A_t [g(t) W_0 \beta_\pi(t) T^2(t) t^{-2}/c + B_\lambda(t) \Omega_{th} \Delta\lambda] + I_{cc}\}},$$

which gives the most complete estimation of the method by the criterion of its noise stability.

Among other factors, which are taken into account, we shall briefly consider the following ones.

Responsiveness of a method is especially important in studying non-steady processes occurring in the atmosphere. By this criterion one should give preference to the methods that allow acquiring information along the entire sounding

path while sending only one sounding pulse. The multipulse methods are naturally less effective.

Reliability. For the optical regulation elements the reliability is determined by stability of the regulation geometric factor $g(z)$, by which the $D_{l.s}$ compression is performed within the interval of its operation, or by the number of elements used for the step-wise regulation. When $D_{l.s}$ is compressed in a photodetector and an amplifier the ordinary methods of estimation of the electronic system reliability apply quite well. On the whole, the reliability is determined by the complexity of the regulating devices.

In exploiting lidars equipped with the devices for the $D_{l.s}$ compression the *design factor, mass, and dimensions* with which *the cost characteristics* of lidar systems are directly connected play an important part.[21] The factors of cost allow one to estimate the performance and cost effectiveness of a device operation during the routine exploitation and the methods of check up of the equipment parameters. The quantitative estimation of the methods using these factors exceeds the bounds of the given paper.

Comparative analysis of the methods

The estimation criteria introduced above allow one to compare the methods of $D_{l.s.}$ compression in the generalized form without fixing the place of allocation of the regulation element in the receiving system and, if necessary, give a possibility of specifying some of its characteristics. Below the methods of functional (compensation for the inverse squared range and logarithmic transformation) and a step-wise regulation are analyzed as being most widely used.

Comparison of the methods by the coefficient of the dynamic range compression

The method of compensation for the inverse squared range (CSR) is the linear transformation relative to the input action $F(t)$. According to Eqs. (1) and (5) $D_{in} = D_{l.s}$. The output action $V(z)$ and output dynamic range D_{out}^{CSR} are determined as

$$[V(z)]_{CSR} = F(z)\, z^2; \tag{13}$$

$$D_{out}^{CSR} = \frac{g(z_i)\,\beta_\pi(z_i)}{g(z_f)\,\beta_\pi(z_i)} \exp\left[2\int_{z_i}^{z_f} \alpha(z)\,dz\right]. \tag{14}$$

And the compression coefficient

$$G_{CSR} = (z_f/z_i)^2 \tag{15}$$

depends only on the range interval z_i–z_f within which the regulation is being performed. As was noted above, the active CSR methods are limited by the maximum value of the input action $F(z_i) < F_{max}$[15,20] causing the saturation of the regulation element. It can be lowered by attenuating $F(z_i)$ with an attenuator placed before a regulation element. Since for $F(z_i) < F_{max}$ the expression (13) is linear relative to $F(z)$, the lower limit for the input action is limited theoretically by the noise level only, $F(z_f) \geq F_n$. In practice, $F(z_f)$ is determined by the range of the regulation having its own limits in optical regulation elements, the photoelectronic[20] or electronic[15] ones.

The method of logarithmic transformation (LT) within the limits of LAC validity is a nonlinear transformation of $F(z)$ and is applied at the high levels of the input signal.[15,22] The low threshold value $F(z_f) = F_{min}$ determines the starting point of a LAC therefore, according to Ref. 15

$$[V(z)]_{LT} = V(z_f)\,\{\ln [F(z)/F(z_f)] + 1\}. \tag{16}$$

At $F(z) < F_{min}$ the LAC becomes linear-logarithmic characteristic, and then at the further decrease of $F(z)$ it becomes the linear one. The dynamic range of a signal at the output of a regulation element and the compression coefficient are equal to

$$D_{out}^{LT} = \ln D_{in} + 1; \tag{17}$$

$$G_{LT} = D_{in}/(\ln D_{in} + 1). \tag{18}$$

One can see from the expression (18) that the LT method allows one to obtain rather large values of G if the value D_{in} of a nonlinear element LAC is large. Since the real logarithmic converters have $D_{in}^{LT} = 10^5$–10^6 (Refs. 15 and 22) then $G_{LTmax} = 8\cdot10^3$–$6.7\cdot10^4$.

The method of step-wise regulation (SR) is realized, as it was noticed above, either by a discrete division of the level of input action or by the discrete regulation of the gain of a regulation element. Figure 2 shows an example of the step-wise regulation when several receiving systems are used to form the total lidar return signal.[16]

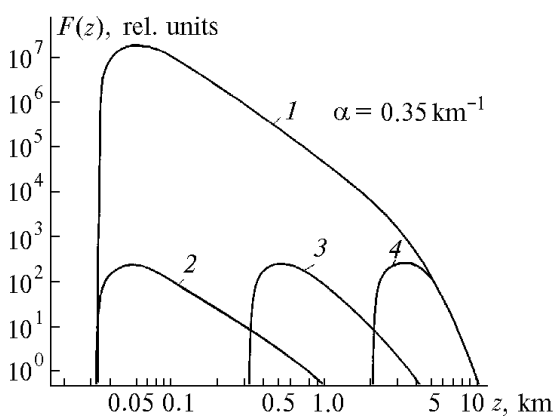

Fig. 2. The step-wise regulation of lidar returns in an optical channel: (*1*) the total flux of backscattered radiation; (*2, 3, 4*) signals at the photodetector input in separate optical receivers.

We shall suppose that for the step-wise regulation the changes of the gain occur at the values of input action $F = F_1, F_2, F_3, \ldots F_n$. Then the ratios

$$D_{in\,1} = F_1/F_i;\ D_{in\,2} = F_2/F_1;\ \ldots D_{in\,n} = F_n/F_{n-1}, \tag{19}$$

where F_i is the initial value of the action in the characteristic

$$[V(z)]_{SRi} = K_i\, F(z) \tag{20}$$

with the linear coefficient K_i of the transmission of the ith step of regulation, will determine the dynamic ranges of separate n steps of the regulation. To make the SR method easy to perform, we assumed that $D_{ini} = D_{outi} = D_{out}$, i.e., every step operates in the identical linear regime (Fig. 3).

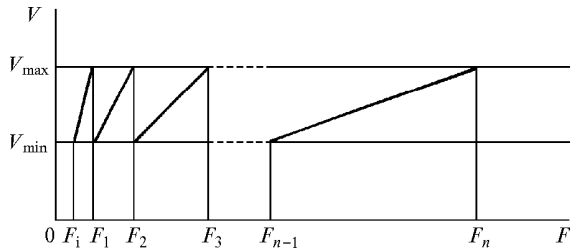

Fig. 3. The step-wise regulation characteristic at a linear conversion in every step.

Then for n steps of the regulation the dynamic range of the device as a whole relative to the input action is

$$D_{in}^{SR} = F_n/F_i = [D_{in\,i}]^n, \quad (21)$$

and the dynamic range at the output (see Fig. 3) is:

$$D_{out}^{SR} = D_{out\,i}. \quad (22)$$

Allowing for expressions (19) to (22), the coefficient of the dynamic range compression is determined as:

$$G_{SR} = [D_{in\,i}]^{n-1} = [D_{out}]^{n-1} = [D_{in}]^{(n-1)/n}. \quad (23)$$

If the dynamic ranges of a single step $D_{in\,i}$ and lidar signal D_{in} are known, then the necessary number of the regulation steps is

$$n = \ln (D_{in}/D_{in\,i}), \quad (24)$$

and the output dynamic range is

$$D_{out}^{SR} = (D_{in})^{1/n}. \quad (25)$$

Let us compare the methods by the value of G that can be attained. Figure 4 shows the dependences (15), (18), and (23).

Since the CSR method in the interval of its application does not depend on D_{in}, the horizontal straight lines represent the values of G_{CSR}. In the region of small values of D_{in} (up to 10^4–10^5) the CSR method provides an attainment of the largest G value. The LT method gives approximately the same value of G as the SR method with 4 or 5 steps. It should be noted that the dependence $G_{LTmax}(D_{in})$ (curve *7*) is correct up to the values $G_{LTmax} = 10^4$ only. The active CSR methods have restrictions of $D_{in} < 10^5$ also. To realize larger values of G at $D_{in} < 10^5$, the SR method with the number of steps determined by the expression (24) or a combination of the SR method with $n = 2$ and the CSR in each step[16] are preferable.

Since the CSR and LT methods have approximately identical upper limit of D_{in}, let us compare them. To simplify analysis, we consider the case of a homogeneous atmosphere and constant values of $\alpha(z)$ and $\beta_\pi(z)$. If the methods are applied to the same range interval z_i–z_f, i.e., for one and the same D_{in}, then, dividing Eq. (18) by Eq. (19), we obtain

$$\frac{G_{LT}}{G_{CSR}} = \frac{\exp\,[2\tau_i\,(z_f/z_i - 1)]}{2\ln(z_f/z_i) + 2\tau_i\,(z_f/z_i - 1)}. \quad (26)$$

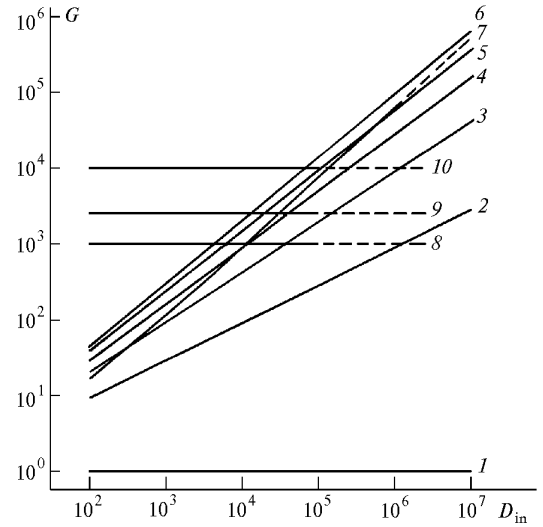

Fig. 4. The values of the compression coefficient for different regulation methods: (*1*–*6*) SR (the curve number corresponds to the number of the regulation steps); (*7*) LT; (*8*–*10*) CSR [(*8*) $G = 10^3$, (*9*) 2500, (*10*) 10^4].

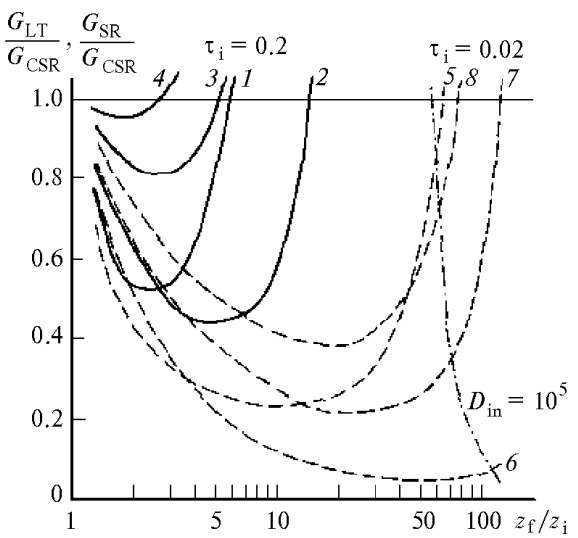

Fig. 5. Relative efficiency of the compression coefficient for the LT and SR methods compared with CSR: (*1*, *5*) LT; (*2*, *6*) SR (for $n = 2$); (*3*, *7*) SR (for $n = 3$); (*4*, *8*) SR (for $n = 4$).

The dependence (26) is presented in Fig. 5 for two values of the optical depth $\tau_i = \alpha z_i$ of the lidar blind zone. One can see from the figure and expression (26) that the LT method is more efficient in strongly turbid media at the small value of z_f/z_i only, when the exponential attenuation introduces the basic contribution to $D_{l.s}$, or at a very large ratio $z_f/z_i > 60$. The dashed-dotted curve sets to the right-hand side boundary of the region $D_{in} > 10^5$ where the limitations noted above apply to the considered methods. Figure 5 also shows the ratio G_{SR}/G_{CSR} obtained under the same assumptions as G_{LT}/G_{CSR}. In the weakly turbid media ($\tau_i < 0.02$) the CSR method is more efficient then the SR method with $n = 4$ over the whole range interval z_i–z_f. However, already at $\tau_i = 0.1$, the SR method becomes more efficient on the short intervals z_i–z_f even at a small number of steps.

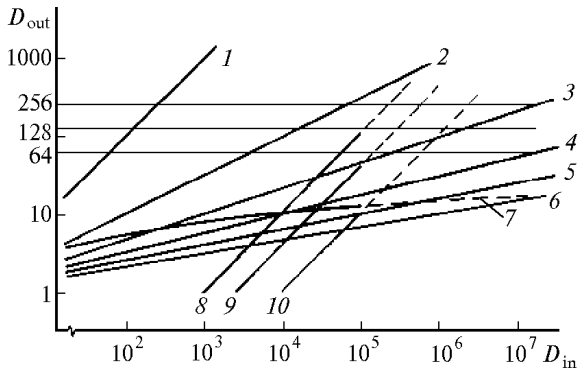

Fig. 6. Comparison of the methods by the attained output dynamic range: (*1–6*) SR (the curve number corresponds to a number of the regulation steps); (*7*) LT; (*8–10*) CSR [(*8*) $G = 10^3$, (*9*) 2500, (*10*) 10^4].

The dependences $D_{out}(D_{in})$ determined by the relations (15), (16), and (17) are shown in Fig. 6. The lines which are parallel to the abscissa axis correspond to three values of D_{in}^{ADC} (6, 7, and 8 bits). The most suitable method to compress $D_{l.s}$ can be chosen proceeding from these dependences at given values of D_{in} and D_{in}^{ADC} allowing for the comments concerning the maximum possible values of $D_{in\ max}^{LT}$ and $D_{in\ max}^{CSR}$ which depend on the properties of the regulation elements. The points of intersection of the dependences *1–10* with the lines of D_{in}^{ADC} determine the theoretically attainable values of the dynamic range of the input lidar return signal $D_{in\,max}$ using the method chosen. These values are presented in Table 2.

Table 2. Comparison of the methods by theoretical $D_{in\ max}$ values

Regulation method			Maximum attainable values of $D_{in\ max}$		
			$D_{in}^{ADC} = 64$	$D_{in}^{ADC} = 128$	$D_{in}^{ADC} = 256$
No regulation ($G = 1$)			$0.640 \cdot 10^2$	$1.280 \cdot 10^2$	$2.560 \cdot 10^2$
SR	$n =$	2	$4.096 \cdot 10^3$	$1.638 \cdot 10^4$	$6.554 \cdot 10^4$
		3	$2.621 \cdot 10^5$	$2.097 \cdot 10^6$	$1.678 \cdot 10^7$
		4	$1.678 \cdot 10^7$	$2.684 \cdot 10^8$	$4.295 \cdot 10^9$
		5	$1.074 \cdot 10^9$	$3.436 \cdot 10^{10}$	$1.099 \cdot 10^{12}$
		6	$6.872 \cdot 10^{10}$	$4.398 \cdot 10^{12}$	$2.815 \cdot 10^{14}$
CSR	$G =$	1000	$6.400 \cdot 10^4$	$1.280 \cdot 10^5$	$2.560 \cdot 10^5$
		2500	$1.600 \cdot 10^5$	$3.200 \cdot 10^5$	$6.400 \cdot 10^5$
		10000	$6.400 \cdot 10^5$	$1.280 \cdot 10^6$	$2.560 \cdot 10^6$
LT			$2.294 \cdot 10^{24}$	$1.430 \cdot 10^{55}$	$5.560 \cdot 10^{70}$

One can see from the data given in Table 2 that the SR method already at $n = 4$ allows one to record lidar returns practically from all atmospheric formations presented in Fig. 1. By the attained value of $D_{in\,max}$ the CSR and SR methods (at $n = 3$) are roughly identical, and for two regulation steps the latter is worse than the CSR method at $G_{CSR} = 10^3$.

Comparison by the relative increase of sounding range

In accordance with the Eq. (9) we will compare three methods by the value of sounding range with the ordinary lidar having D_{in}^{l} under the condition that ADC has the same D_{in}^{ADC}

$$D_{in}^{l} = D_{out}^{LT} = D_{out}^{CSR} = D_{out}^{SR} = D_{in}^{ADC}. \quad (27)$$

We will consider that the methods start to operate at the same value of the input action $F(z_i)$ and the equality (27) is satisfied in the intervals $z_i - z_{f.l}$, for ordinary lidar, $z_i - z_{f.LT}$, for LT, $z_i - z_{f.CSR}$ for CSR, $z_i - z_{f.SR}$ for SR (with $n \geq 2$). To simplify analysis, we assume the atmosphere to be homogeneous along the sounding path.

In the absence of regulation ($G = 1$), assuming $D_{in} = D_{l.s}$, we have from Eqs. (27) and (1) for an ordinary lidar that

$$\ln(z_{f.l}/z_i) + \tau_i (z_{f.l}/z_i - 1) = 0.5 \ln D_{in}^{ADC}. \quad (28)$$

By analogy with the relations (17), (14), and (25) we obtain for the LT, CSR, and SR methods

$$\ln(z_{f.LT}/z_i) + \tau_i (z_{f.LT}/z_i - 1) = 0.5(D_{in}^{ADC} - 1); \quad (29)$$

$$\tau_i (z_{f.CSR}/z_i - 1) = 0.5 \ln D_{in}^{ADC}; \quad (30)$$

$$\ln(z_{f.SR}/z_i) + \tau_i (z_{f.SR}/z_i - 1) = (n/2) \ln D_{in}^{ADC}. \quad (31)$$

At $n = 1$ the expression (31) reduces to expression (28). One can see from the Table 2 that the theoretical values of $D_{in\,max}$ for LT method exceed the values of $D_{in}^{LT} = 10^5 - 10^8$ that can be obtained in practice therefore the estimation $(\delta z)_{LT}$ was performed for $D_{in}^{LT} = 10^5$ from the equation (29) modified to following form

$$\ln(z_{f.LT}/z_i) + (z_{f.LT}/z_i - 1) = 0.5 \ln(D_{in}^{ADC} - 1). \quad (32)$$

To determine the relative increase in the sounding range $(\delta z)_{LT} = z_{f.LT}/z_{f.l}$, $(\delta z)_{CSR} = z_{f.CSR}/z_{f.l}$, and $(\delta z)_{SR} = z_{f.SR}/z_{f.l}$, it is necessary to solve jointly the equations (28), (30), (31), and (32). The results of their numerical solution are presented in Fig. 7.

Since $D_{l.s}$ is a function of z^{-2} and extinction coefficient α, the dependences (δz) are presented as functions of $\tau_i = \alpha z_i$, and two values of D_{in}^{ADC} equal to 64 and 128 characteristic of most common ADCs. Such a representation of the dependences (δz) allows one to analyze the methods of $D_{l.s}$ compression regardless of the blind zone length z_i and different values of the extinction coefficient α.

On can see from Fig. 7 (curves *1* and *1′*) that allowing for the realistically limited value of D_{in}^{LT} the increase in D_{in}^{ADC} does not cause an increase in the relative sounding range. Therefore it is not necessary to use ADCs with large value of D_{in}^{ADC} in the lidars with LAC regulation elements.

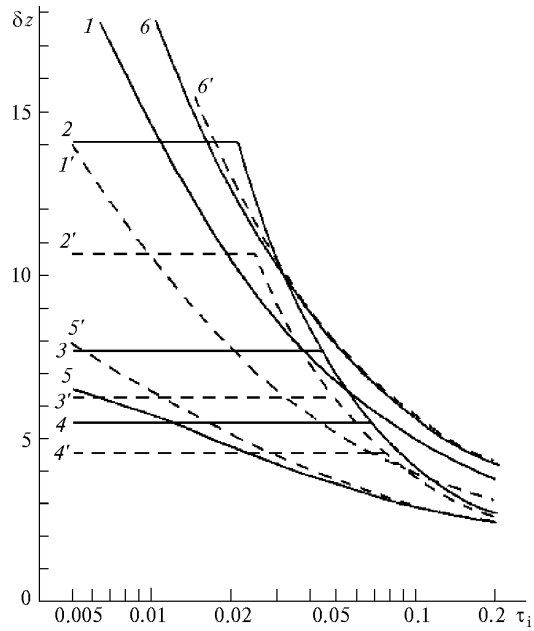

Fig. 7. The relative increase in sounding distance for three methods to compress the dynamic range at the $D_{in}^{ADC} = 64$ (solid lines), $D_{in}^{ADC} = 128$ (dashed lines): (*1*, *1′*) LT; (*2–4* and *2′–4′*) – CSR [(*2*) $G = 10^4$, (*3*) 2500, (*4*) 10^3]; (*5*, *6* and *5′*, *6′*) SR [(*5*) $n = 2$, (*6*) $n = 3$].

It is typical for the CSR method that $(\delta z)_{CSR}$ decreases with the increasing D_{in}^{ADC}, since in this case the interval $z_i - z_{f.l}$ increases more quickly then the interval $z_i - z_{f.CSR}$. Since in an actual lidar the ratio $z_{f.CSR}/z_i$ is limited in accordance with (15) by the value G_{CSR} depending on the properties of a compensating element then there exists a limit of the $(z_{f.CSR}/z_i)$ maximum

$$(z_{f.CSR}/z_i)_{max} \le (G_{CSR})^{1/2}, \qquad (33)$$

after this limit compensation for the inverse squared range stops and the regulation element passes to the linear regulation mode of operation (PMT with TDA or amplifier with TDA) or to a more complex (for spatial filters) regulation mode. Therefore the ratio $z_{f.CSR}/z_i$ remains constant after the regulation termination. Inflection points on the curves *2 – 4* and *2′ – 4′* (see Fig. 7) are determined by substituting expression (15) into the Eq. (30) from the condition

$$\tau_i = \ln D_{in}^{ADC}/2[(G_{CSR})^{1/2} - 1]. \qquad (34)$$

Table 3 gives the values $(\delta z)_{CSR.max}$ corresponding to the inflection points. These values are attainable in a weakly turbid atmosphere or at small lengths of the blind zones. When τ_i grows, the values of $(\delta z)_{CSR}$ decrease that is caused by the increasing weight of the exponential factor in the dynamic of a lidar return which is not compensated for in this method.

The SR method at $n = 2$ leads to an increase in $(\delta z)_{SR}$ with the increasing D_{in}^{ADC} although this difference decreases with the growth of τ_i. But already at $n \ge 3$ the increase in D_{in}^{ADC} does not essentially affect the change of $(\delta z)_{SR}$ that is caused by a more rapid growth of $z_{f.l}/z_i$ as compared with $z_{f.SR}/z_i$ at large values of D_{in}^{ADC}. In the region $\tau_i \ge 0.1$ the value of $(\delta z)_{SC}$ increases linearly with the growth of the number of steps, and in the less dense medium this increase is nonlinear.

Table 3. Maximum values of the relative increase of the sounding range at a compensation for the inverse squared range dependence of the lidar returns

D_{in}^{ADC}	$(\delta z)_{CSR\ max}$		
	$G = 10^3$	$G = 2{,}5 \cdot 10^3$	$G = 10^4$
64	5.5	7.7	14.1
128	4.6	6.3	10.9
256	3.9	4.8	8.4

One can see from Fig. 7 that at $D_{in}^{ADC} = 128$ the strongest effect, for all atmospheric situations, is provided by the SR method (at $n \ge 3$) then the CSR method follows (in the interval $0.01 \le \tau_i \le 0.09$ for $G_{CSR} = 10^4$ and in the interval $0.03 \le \tau_i \le 0.09$ for the $G_{CSR} = 2.5 \cdot 10^3$), and then follows the LT method. The SR method at the $n = 2$ has an advantage in the region of small τ_i only when the limited value of the ratio $z_{f.CSR}/z_i$ which is determined by the relationship (34) does not provide the compensation for z^{-2} along the entire sounding path. The use of the six-bit ADC ($D_{in}^{ADC} = 64$) gives different picture of δz. In this case the CSR method at the $G_{CSR} = 10^4$ has certain advantages in the increase of the relative sounding range δz even in comparison with the SR method (at $n \ge 3$) in the region $0.016 \le \tau_i \le 0.032$ and with the LT method in a more wide region of τ_i values.

Comparison of the methods by the dynamic signal-to-noise ratios

In modern PMTs the equivalent threshold power is determined by the first and second terms in the denominator of the expression (12) therefore the effect of the PMT's dark current can be neglected. Considering, for simplicity, the atmosphere along the sounding path to be homogeneous and that the background brightness does not change during the measurements, let us present the expression for the dynamic signal-to-noise ratio as[8]

$$D_{SN}(t) = \frac{S_{\lambda c}\,[A_c\,K_1(t)\,\beta_\pi\,T(t)\,t^{-2}]^2}{2e\Delta f\,[A_c\,K_1(t)\,\beta_\pi\,T(t)\,t^{-2} + A_b\,K_2(t)\,B_\lambda]}, \qquad (35)$$

where A_c takes into account the instrumental constants in the lidar equation; A_b takes into account the instrumental constant of the receiving system in the passive regime of the background radiation recording; $K_1(t)$ is the transmission coefficient of the receiving system which takes into account the geometric function; $K_2(t)$ is the transmission coefficient of the optical system for the background radiation.

One can see from Eq. (35) that $D_{SN}(t)$ does not depend on $M(t)$, i.e., the regulation in PMT does not change the value of the dynamic signal-to-noise ratio because the fluxes of the backscattered and background radiation are subjected to identical transformations. This conclusion is correct only up to the power level of these radiations when $I_s(t)$ and $I_b(t)$ do not essentially affect the redistribution of the electric current over the PMT voltage divider. Analogous conclusion about the invariability of the signal-to-noise ratio can be obtained for the regulation of the gain in the electronics of the lidar too. The regulation in the

optical part of the receiving system changes the signal-to-noise ratio.

The laws of change of the coefficient $K_i(t)$ depend on the method of $D_{l.s}$ compression used. For the optical CSR method we have

$$K_1(t) = \begin{cases} 0, & t_0 \ge t \ge 0 \\ f(t), & t_i \ge t \ge t_0 \\ K_0(t/t_i)^2, & t_f \ge t \ge t_i \end{cases}, \quad (36)$$

where t_0 is the time corresponding to the far end of the lidar blind zone, t_i and t_f are the moments of the start and termination of the regulation process, $f(t)$ is the transmission coefficient of a spatial filter in the transition zone[10] which determines the leading edge of a lidar return pulse; K_0 is the value of the transmission coefficient of a receiving system in the beginning of the regulation process.

For the SR method with three steps we have

$$K_1(t) = \begin{cases} K_{S1}, & t_{f1} \ge t \ge t_{i1} \\ K_{S2}, & t_{f2} \ge t \ge t_{i2} \\ K_{S3}, & t_{f3} \ge t \ge t_{i3} \end{cases}. \quad (37)$$

In this case $K_{S1} \le K_{S2} \le K_{S3}$, and the moments of the initial time $t_{i,i}$ and final time $t_{f,i+1}$ of the regulation in different steps can have different relations depending on the specific operation of the method. In the lidar which has several receivers it is necessary to choose $t_{f1} > t_{i2}$.

For spatial filters compensating for the inverse squared range dependence the transmission for backscattered radiation flux changes according to the relation (36) by the movement of the image spot relative to this element,[10] while the background radiation flux passes through the whole element and does not change with time, i.e., $K_2(t) = K_b$. Thus, for the functional regulation in the optical part and at $t_f \ge t \ge t_i$ we have

$$D_{SN}(t) = \frac{S_{\lambda c}\,[A_c\,K_0\,\beta_\pi\,T^2(t)\,t_i^{-2}]^2}{2e\Delta f\,[A_c\,K_0\,\beta_\pi\,T^2(t)\,t_i^{-2} + A_b\,K_b\,B_\lambda]}. \quad (38)$$

By comparing Eqs. (35) and (38) we see that in the second case $D_{SN}(t)$ depends on the time much more weakly. Under night conditions ($B_\lambda = 0$) it is

$$D_{SN}(t) \sim [T(t)]^2, \quad (39)$$

and under daytime conditions (the second term in the denominator in (38) prevails) it is

$$D_{SN}(t) \sim [T(t)]^4. \quad (40)$$

Whereas in the absence of the regulation from Eq. (12) we have $D_{SN}(t) \sim [T(t)/t]^2$, in the first case, and in the second case we have $D_{SN}(t) \sim [T(t)/t]^4$ (see, for example, Ref. 1).

For the optical SR methods within one step $D_{SNi}(t)$ changes during the time as in ordinary lidar according to the relation (35) since in this case $K_1(t) = K_{Si}$, $K_2(t) = K_{bi}$ where the step number is $i = 1, 2, 3$. However, for far parts of the path one always choose $K_{b1} < K_{b2} < K_{b3}$ by decreasing the field-of-view angle of the receiving system.[16] Therefore even for $K_{S1} = K_{S2} = K_{S3}$ the value $D_{SN2}(t)$ at the beginning of the second step exceeds the value $D_{SN1}(t)$ at the end of the first step, and by the choosing properly K_{bi} and K_{Si} it can be attained

$$D_{SN1}(t_{f1}) \approx D_{SN2}(t_{f2}) \approx D_{SN3}(t_{f3}). \quad (41)$$

Thus, the value $D_{SN3}(t_{f3})$ will exceed to a considerable degree the value of the dynamic signal-to-noise ratio for a hypothetical lidar which does not use any method of the $D_{l.s}$ compression at the same range $z_{f.G}$.

Analysis carried out shows that the optical methods of $D_{l.s}$ compression allow one to improve the signal-to-noise ratio by more than an order of magnitude and, based on this improvement, to increase the sounding range and the accuracy of lidar measurements.

Estimation of the error of signal conversion at the regulation

The type of regulation element used to compress $D_{l.s}$ essentially affects the accuracy of information that is retrieved from a lidar return signal. If we assume that all elements of the receiving system operate in a linear mode then the error in the recorded lidar information will be determined completely by the error of recording device, for example, by the errors of digitizing with an ADC. Therefore the SR methods where photoelectronic and electronic channels operate in a linear mode have the least conversion error. In the case when the step-wise regulation is performed by discrete change of the gain as it is realized, for example, in PMT[23] or in amplifier[24] a partial loss of information occurs at the moments of step-wise switching of the gain from one range to another. The SR method in the optical channel composed of several receiving systems[16] is the most admissible, when the photoelectronic and other parts of every receiving system operate within the same dynamic range. However, in this case it is necessary to make intercalibration of the receiving systems in the overlapping parts of the sounding path (see Fig. 2).

For the CSR methods the error in the gain exists due to deviation of the regulation characteristic from the exact square law $\varphi[F(z)] = az^2$. The relative error (at a constant regulation characteristic) is the function of range

$$\delta V(z) = \{f\,[F(z)]_{CSR} - az^2\}/az^2, \quad (42)$$

where a is the constant; $f\,[F(z)]_{CSR}$ is the actual characteristic of the regulation element. If the errors $\delta V(z)$ and $\Delta V(z)$ are constant on the interval of the regulation z_i–z_f, i.e., the mean constant value of the deviation $\Delta V(z_i)$ exists for every sounding range then it can be taken into account by the introducing the coefficient

$$K(z_i) = a(z_i)^2/f\,[F(z_i)], \quad (43)$$

when the ordinates of the lidar return signal digitized in an ADC are multiplied by this coefficient during the processing in a computer. Thus, correction for the error of the regulation characteristic can be done there. For the optical regulation elements this correction is valid if no misalignment of optical axes occurs and a structure of laser radiation spot does not change from pulse to pulse. For the active regulation elements the correction (43) is valid if the value $F(z_i)$ does not exceed the values that make the PMT with TDA or an amplifier with TDA to operate in a nonlinear mode.

It is a more complicated task to take into account the deviations of amplitude of the regulation characteristic of the LT method from the theoretical relationship (16) since the actual $[V(z)]_{LT}$ has the parts with different functional dependence $V = f(F)$.[15] One has to maintain certain levels of input signals to meet the LAC regulation characteristic on the corresponding intervals of the sounding path.

However, depending on the atmospheric conditions, the value β_π can vary by the several orders and for this reason the value of a signal in the near zone of a lidar varies within two or more orders of magnitude (see Fig. 1). Therefore LT method can give large errors during the information processing.

Comparison according to other estimation criteria

It is difficult to make generalized quantitative analysis of the $D_{l.s}$ compression methods by the responsiveness, reliability, and other proposed criteria since it is necessary to take into account directly the type and parameters of the regulation elements. In some necessary cases analysis can be carried out using these criteria in considering the operation of a particular regulation element.

The functional methods of $D_{l.s}$ regulation in optical channel of a lidar should be referred to the most simple and inexpensive methods. The SR method with the change of field-stop diaphragms is also easy to perform, but it is not efficient because requires an additional time to change the diaphragms. A lidar with several receiving systems is highly efficient but it is too complex in design.

In the photoelectronic channel a preference should be given to PMTs with TDA of the functional or step-wise type of the amplification regulation. Among the electronic regulators the amplifiers with the step-wise switching of the gain are preferable.

Conclusion

The principles of classification of the methods and devices of $D_{l.s}$ compression considered allow one to systematize practically all existing techniques of regulating the dynamic range of lidar return signals. The proposed set of criteria to estimate the efficiency of these methods provides for their generalized analysis to be made. The compression of $D_{l.s}$ in optical part of a receiving system increases the signal-to-noise ratio by several times. The use of functional elements compensating for the inverse squared range dependence in a wide interval sounding range ($z_f/z_i = 100$) allows one to increase considerably (by a factor of 10) the sounding range that is comparable with the systems having three steps of the regulation.

The development of fast ADC's with the large input dynamic range (10 – 12 bits at the clock rate of 100 to 200 MHz) allows one to record lidar returns in the analog mode with smaller distortions that is especially important for the space-based lidar sounding.

References

1. C.A. Northend, R.C. Honey, and W.E. Evans, Rev. Sci. Instr. **37**, No. 4, 393–400 (1966).
2. A.I. Abramochkin and A.A. Tikhomirov, *Instrumentation and Methods of Remote Sensing of Atmospheric Parameters* (Nauka, Novosibirsk, 1980), pp. 19–29.
3. A.A. Tikhomirov, in: *Forecast and Regulation of Optical-Meteorological Conditions of the Atmosphere* (Publishing House of the Institute of Atmospheric Optics, Tomsk, 1982), pp. 47–53.
4. V.E. Zuev, I.V. Samokhvalov, and A.A. Tikhomirov, *Abstracts of Papers at the 12th International Laser Radar Conference*, Aix-en Provence, France (1984), pp. 75–77.
5. A.A. Tikhomirov, in: *Abstracts of Reports at the VIIth All-Union Symposium on Laser and Acoustic Sounding of the Atmosphere*, Tomsk, (1982), Part II. pp. 169–172.
6. A.A. Tikhomirov, in: *Abstracts of Reports at the VIIIth All-Union Symposium on Laser and Acoustic Sounding of the Atmosphere*, Tomsk, (1984), Part II. pp. 283–286.
7. A.A. Tikhomirov, in: *Abstracts of Reports at the VIth All-Union Symposium on Laser and Acoustic Sounding of the Atmosphere*, Tomsk, (1980), Part II. pp. 58–61.
8. A.A. Tikhomirov, in: *Abstracts of Reports at the VIIIth All-Union Symposium on Laser and Acoustic Sounding of the Atmosphere*, Tomsk, (1984), Part II. pp. 287–290.
9. A.A. Tikhomirov, *Measurement of Optical and Meteorological Parameters of the Atmosphere Using Laser Radiation* (Publishing House of the Institute of Atmospheric Optics SB AS USSR, Tomsk, 1980), P. 106–114.
10. A.I. Abramochkin and A.A. Tikhomirov, Atmos. Oceanic Opt. **12**, No. 4, 331–342 (1999).
11. A.I. Abramochkin and A.A. Tikhomirov, *Problems in Remote Sensing of the Atmosphere* (Publishing House of the Institute of Atmospheric Optics SB AS USSR, Tomsk, 1976), pp. 21–32.
12. I.I. Anisimova and B.M. Glukhovskoi, *Photomultiplier Tubes* (Sov. Radio, Moscow, 1974), p. 64.
13. A.V. Pavlov, *Optoelectronic Devices (Principles of Theory and Calculation)* (Energiya, Moscow, 1974), 360 pp.
14. L.S. Gutkin, *Optimization of Radio-Electronic Devices by the Set of Performance Indices* (Sov. Radio, Moscow, 1975), 388 pp.
15. V.M. Volkov, ed., *Functional Amplifiers with Large Dynamic Range. Principles of Design and Calculation.* (Sov. Radio, Moscow, 1976), 334 pp.
16. A.I. Abramochkin, Yu.S. Balin, P.P. Vaulin, A.F. Kutelev, I.V. Samokhvalov, and A.A. Tikhomirov, *Measurement Instrumentation to Study Parameters of Surface Layers of the Atmosphere* (Publishing House of the Institute of Atmospheric Optics SB AS USSR, Tomsk, 1977), pp. 5–16.
17. Yu.S. Balin, I.V. Samokhvalov, and V.S. Shamanaev, *"Method of optical sounding of the atmosphere,"* Inventor's Certificate No. 496524, Bull. No. 47, 1975.
18. V.A. Kovalev, Trudy Gl. Geofiz. Obs. Issue 357, 121–133 (1976).
19. Yu.S. Balin, V.P. Galileiskii, I.V. Samokhvalov, and V.S. Shamanaev, *Problems in Laser Sounding of the Atmosphere* (Nauka, Novosibirsk, 1976), pp. 34–45.
20. A.I. Abramochkin, P.M. Nolle, and A.A. Tikhomirov, in: *Proc. of the 9th Intern. Symp. on the TC-2 and Photon-Detectors*, IMEKO, Hungary (1980), pp. 92–99.
21. Z.K. Pratt, *Laser Communication Systems* (Svyaz', Moscow, 1972), 232 pp.
22. V.V. Bacherikov, Yu.A. Makarov, Yu.N. Nikolaev, and B.M. Stepanov, Prib. Tekh. Eksper. No. 4, 147–150 (1974).
23. R.R. Agishev, G.I. Il'in, Yu.E. Pol'skii, Prib. Tekh. Eksper. No. 4, 199–202 (1981).
24. J.D. Spinhirne, J.A. Reagan, Rev. Sci. Instrum. **47**, No. 4, 437–439 (1976).